BBXRT Low Energy Background Subtraction

Kimberly Weaver

December 11, 1992

1 The Atmosphere and the X-ray-bright Earth

Goddard's Broad Band X-ray Telescope flew as part of the Astro-1 mission aboard the space shuttle *Columbia* in December 1990. The shuttle's orbit places it in the Earth's upper atmosphere (the ionosphere[1]) at an altitude of ~200 km. Because low energy x-rays are absorbed and scattered at such altitudes, observations of celestial sources will be affected. It is therefore important to have an accurate understanding of the composition and ionization state of the atmosphere.

Between sea level and an altitude of 90 km, the Earth's atmosphere is comprised mostly of N_2 (78%) and O_2 (21%) (Jones 1964). At 90 km, photodissociation of O_2 begins and O exceeds O_2 at an altitude of ~110 km. This is illustrated in Figure 1, taken from Mitra (1952) which shows the particle density as a function of height for molecular and atomic oxygen. Molecular nitrogen begins dissociation around 150-200 km (Zombeck 1990) but the process is complicated and there is no specific level where N_2 is mostly dissociated. At the height of the space shuttle orbit (~200 km) nitrogen still exists mainly in molecular form (Zombeck 1990, Mitra 1952) and the ratio of O to N_2 is approximately 1:1 (Zombeck 1990). In addition, the upper atmosphere can be treated as neutral because at no time do the ions exceed more than 1% of their corresponding neutral species up to 700 km (Jones 1964).

BBXRT suffers from a large amount of low energy (0.3-1.0 keV) contamination during "day-side" observations. This contribution to the x-ray background occurs when the shuttle passes

[1]The ionosphere extends between altitudes of 60-700 km. The free electrons in the ionosphere, which affect radio wave propagation, are liberated from the ionization of gases by solar UV and X-rays.

over the Sun-lit Earth, and is created by x-ray photons from the solar corona which scatter from the molecules and atoms in the Earth's upper atmosphere. The relevant scattering processes involved are Thomson scattering and fluorescent scattering. By modeling the radiative transfer of x-rays through the Earth's atmosphere, Snowden and Freyberg (1993) and Fink, Schmitt, and Harnden (1988) have determined that observed x-ray "bright Earth" lightcurves and spectra can be accounted for by a variety of different viewing angles. In addition, the observed changes in hardness ratio indicate a change in the ratio of Thomson to flourescently scattered photons as a function of zenith angle (the Sun-Earth-satellite angle).

Thomson scattering is the elastic scattering of photons from the valence electrons of atmospheric atoms, and is the dominant scattering process for energies greater than ~0.6 keV. The modified Thomson cross section can be written as (Fink, Schmitt, and Harnden 1988):

$$\sigma_{mT}(\lambda, Z, \phi)d\Omega = \frac{3}{16\pi}\sigma_T\left[\left(\sum_1^Z f_n\right)^2 + Z - \sum_1^Z f_n^2\right](1 + cos^2\phi)d\Omega$$

where $(\sum_1^Z f_n)^2 = F(\lambda, sin(\phi/2))$ is the atomic structure factor, $\sum_1^Z f_n^2 = G(\lambda, sin(\phi/2))$ is the electronic structure factor, σ_T=6.65 $\times$ 10^{-25} cm^2 is the Thomson cross section and ϕ is the scattering angle. The cross section σ_{mT} is about 5 $\times$ 10^{-24} cm^2 sr^{-1} for oxygen and nitrogen (Fink, Schmitt, and Harnden 1988).

X-ray photons with energies greater than the ionization threshold are absorbed in the atmosphere by photoelectric absorption. The photoionized atoms can then isotropically reemit fluorescence photons. The fluorescent scattering cross section can be written as:

$$\sigma_{sc,fl}(\lambda)d\Omega = y_{fl}(\kappa_{abs}(\lambda)/4\pi)d\Omega$$

where y_{fl}, the fluorescence yields of the K shell for oxygen and nitrogen, are 0.0047 and 0.0077 respectively (Bambynek et al. 1972). The energies of the K absorption edges are 0.537 keV and 0.400 keV for atomic oxygen and nitrogen with the corresponding Kα lines at 0.525 keV and 0.392 keV[2]. The value of the flourescent cross section is of the order of

[2]For the test18 matrix gain adjustment we have chosen atomic oxygen fluorescence to be at 0.525 keV however there exist discrepancies in the literature as to the correct values for the K-edge energy. Bearden and Burr (1967) find the threshold energy (E$_K$) for photoejection of an electron from the K shell to be 0.532 keV which places the edge at ~0.537 keV. The energy of the Kα flourescence line is given by Bearden (1967) to be 0.525 keV. These are the values most often quoted in the literature. However, Gould and Jung (1991) calculate E$_K$ for atomic oxygen to be 0.546 keV. Scaling up the fluorescence line by the same amount places it at 0.540 keV. This would give us a remaining offset of 15 eV in the gain.

10^{-22} cm^{2}sr^{-1} for both oxygen and nitrogen (Fink et al. 1988). For oxygen, the ratio of the scattered and absorption cross sections are $\sigma_{mT}/\sigma_{abs} \sim 1 \times 10^{-5}$ and $\sigma_{fl}/\sigma_{abs} \sim 1 \times 10^{-4}$.

A combination of inaccurate pointing positions and low source yield during the BBXRT mission make it crucial to understand the low energy bright Earth contamination since it is not desirable to throw away source data. There are essentially two states of bright Earth emission, an "active" state when the Sun is flaring and a "quiet" state when the Sun is more or less quiescent. During the active state, we see higher energy emission lines (Mg, Si, Ar) due to the harder spectrum of the Sun as well as a strong thermal continuum and Fe L emission. A spectrum of a typical flare is shown in Figure 2. Luckily, no flares occurred during daytime source observations. During the quiet state, we see mostly scattered Fe L emission from the Sun as well as O and N_2 fluorescence lines. The intensity is dependent upon the Earth limb angle, defined as the angle between the telescope pointing direction and the center of the Earth. A spectrum of the bright Earth obtained for a range of angles 30-50 degrees is shown in Figure 3a. Figure 3b shows the weaker spectrum obtained for the range 80-90 degrees and illustrates how the Thomson scattered continuum dies away as we go to larger angles.

To investigate how the low energy count rate correlates with Earth limb angle, background subtracted count rates (counts cm^{-2} sec^{-1}) for 3 channel ranges were extracted. Figure 4a shows the change in count rate in channels 27-42 (0.5-0.6 keV) vs. angle, chosen to emphasize the oxygen line. The oxygen line is brightest between 70-80° corresponding to the limb angle of the Earth's horizon (~76°) as seen from 200 km. There is a large drop in count rate above 80° although oxygen contamination persists up to 150°. Figure 4b emphasizes the change in Fe L count rate with angle (channels 45-80). A corresponding increase in count rate at 70° is not seen here, however there is once again a rapid drop above 80° with significant counts to an angle of 100°. Figure 4c emphasizes higher energies (channels 80-120: 1-2 keV). The same drop above 70-80° occurs with essentially no contribution in this energy band above 80°.

2 The Internal and Diffuse X-ray Background

All of the following discussion pertains to non-SAA data extracted using *chip_2ms* to remove microphonics.

For nighttime source observations and Earth angles greater than 90°, the background at low energies has two major components, internal and diffuse sky background. The internal detector background, due to electronic noise and particle events, is known to scale ~ linearly with the detector guard rate[3] (see Figure 5) for low guard rates (i.e. < 2000). This correlation has been addressed in previous memos (see Marshall 1991a and Yamauchi 1991). The internal component to the background can be easily predicted and the recommended procedure is to scale an internal background file (mean guard rate MGR=1259) to match a source average guard rate (SGR) by using the background scaling factor *BSF* in *chanpha*, where *BSF = 1259/SGR* (Marshall memo 1991b).

Internal background files with no guard rate cutoffs applied have been created and are available. During the accumulation time there were no passages through the South Atlantic Anomaly (SAA) and the guard A rate varied from ~800 to ~2300. The files are presently located in in /home/chaupher/kim/back/INTERNAL_dir and are called back855... and back855_2ms... The internal background reaches a lower threshold at a guard rate of 1000 and should not be scaled below this value. This can be inferred from Figure 5, a plot of guard rate vs. A1-A4 count rate reproduced from a previous calibration memo (Yamauchi 1991).

Although the diffuse x-ray background makes up no more than 10% of the total background at energies greater than 2 kev, it can be a significant contribution to the total background at lower energies. The count rate in the diffuse background can be as much as 1/2 the internal background count rate between 0.6-1.0 keV and can approximately equal the internal background count rate between 0.4-0.6 keV. Background files have been created consisting of the diffuse nighttime background (average Earth angle 120°) minus the internal background scaled to the nighttime mean guard rate (MGR=1274). These night background files were extracted to have the Earth limb angles greater than 90° and are located in /home/chaupher/kim/back/NIGHT_dir, named nightbacka0... The associated scaled internal background files are called night_back855_2ms... The files are applicable for modeling the shape of the diffuse background and for nighttime background subtraction for Earth angles greater than 90°.

3 Daytime External X-ray Background

As previously stated, the low energy daytime external background is often strong and varies with the telescope position with respect to the Earth. Cleaned daytime, non-SAA, non-solar flare background files have been accumulated for various ranges of Earth limb angles. The earthglow count rate remains constant for guard rates from 800-1800 in a given Earth angle range (see Figure 6), in contrast to the linear correlation seen between count rate

[3]The guard rate is a housekeeping parameter which indicates the rate of particle interactions with the plastic scintillator surrounding most of the detector (Jahoda et al. 1991).

and guard rate for the internal detector background. In order to examine the shape of the daytime bright Earth spectra, diffuse background plus scaled internal background files were subtracted and data for each range of Earth angles (ea) were modeled using *xspec*. The mean guard rates (no GR cutoffs applied) for the extracted daytime non-SAA background files are listed in Table 1. Column 3 contains the background scale factors used to scale the corresponding internal background files.

Table 1		
	MGR	BSF
ea30_50	1066	1.181
ea50_70	1060	1.188
ea70_80	1033	1.219
ea80_90	1229	1.024
ea90_100	1126	1.118
ea100_110	1228	1.025
ea110_120	1210	1.041
ea120_130	1209	1.041
ea130_150	1225	1.028
ea150_180	1010	1.247

4 Procedure: Maximum likelihood analysis

In dealing with few counts and weak sources, the best approach is to use maximum likelihood statistics. In fitting the data, the background is modeled along with the source, therefore one needs to know the appropriate model to use.

Earth Angles 100-150°

For large average Earth limb angles (between 100-150°), the only major daytime contaminant is the atomic oxygen fluorescence line at 0.525 keV. To determine the strength of this feature for a given range of angles bright Earth data were accumulated in each range and then fit after internal and diffuse background subtraction with a gaussian with zero width. The best fit O line energies are given in Table 2, column 1 and were determined using the brightest daytime data (70-80° range). The normalizations of the oxygen line for Earth angles 100-150° (using the test18 matrix) are listed in Table 2 and represent the total contribution of the daytime scattered background at each range of angles. Figure 7 illustrates the fits to the oxygen line for the data in the 100-110° range. To correctly model the background for a daytime observation, one can either subtract off the internal component and model the diffuse component (see Jahoda et al. 1991) and the oxygen line, or model both the diffuse plus internal background and the oxygen line. Notice that the gain is still off in pixel B3 by about 25 eV at low energies.

Table 2: Fits to Oxygen line

pixel	line energy	ea100_110	ea110_120	ea120_130	ea130_150
	keV	norm	norm	norm	norm
a0	0.526 ± 0.002	0.0011 ± 0.0002	0.0007 ± 0.0002	0.0004 ± 0.0002	0.0003 ± 0.0001
a1	0.516 ± 0.004	0.0034 ± 0.0002	0.0020 ± 0.0003	0.0010 ± 0.0002	0.0008 ± 0.0002
a2	0.525 ± 0.003	0.0027 ± 0.0002	0.0016 ± 0.0003	0.0006 ± 0.0003	0.0007 ± 0.0002
a3	0.524 ± 0.003	0.0031 ± 0.0003	0.0018 ± 0.0003	0.0010 ± 0.0004	0.0009 ± 0.0001
a4	0.532 ± 0.003	0.0057 ± 0.0005	0.0033 ± 0.0006	0.0016 ± 0.0004	0.0019 ± 0.0004
b0	0.526 ± 0.002	0.0012 ± 0.0002	0.0009 ± 0.0003	0.0004 ± 0.0002	0.0002 ± 0.0001
b1	0.524 ± 0.003	0.0012 ± 0.0002	0.0006 ± 0.0003	0.0005 ± 0.0002	0.0003 ± 0.0001
b2	0.526 ± 0.003	0.0025 ± 0.0003	0.0014 ± 0.0005	0.0007 ± 0.0003	0.0006 ± 0.0002
b3	0.541 ± 0.004	0.0045 ± 0.0005	0.0027 ± 0.0006	0.0014 ± 0.0005	0.0012 ± 0.0004
b4	0.518 ± 0.004	0.0024 ± 0.0003	0.0013 ± 0.0003	0.0008 ± 0.0003	0.0006 ± 0.0002

*NOTE: To properly fit the a0 data an additional gaussian is required at 0.392 keV with a norm of 0.0012 ± 0.0005. The values in this table apply only when using the test18 matrix.

Earth Angles 80-100°

For Earth angles between 80-100°, the modeling becomes more complicated. The major features in the background spectra are nitrogen and oxygen flourescence and a broad component centered around 0.8 keV; presumably scattered Fe L emission from the Sun. As before, the best fits for all pixels were determined using the 70-80° data and the norms for each component were found (see Table 3) using internal and diffuse background subtracted spectra for the Earth angle ranges 80-90° and 90-100°. The best description of the data is a Raymond-Smith continuum with 0.05 solar abundance and two gaussians. The oxygen line energy was fixed at the values listed in Table 2. The a4 and outer B pixel effective areas are not reliable at energies less than 0.5 keV (see Weaver 1992 cal memo) so it is not necessary to include a nitrogen line for these pixels.

Table 3: Fits to Raymond plus O,N				
ea80_90				
pixel	kT	norm	O norm	N_2 norm*
a0	0.47 ± 0.05	0.0011 ± 0.0002	0.0096 ± 0.0004	0.011 ± 0.001
a1	0.42 ± 0.02	0.0032 ± 0.0004	0.0270 ± 0.0007	0.033 ± 0.013
a2	0.41 ± 0.02	0.0042 ± 0.0004	0.0233 ± 0.0006	0.040 ± 0.010
a3	0.42 ± 0.02	0.0037 ± 0.0005	0.0240 ± 0.0006	0.045 ± 0.011
a4	0.40 ± 0.03	0.0049 ± 0.0006	0.0440 ± 0.0015	0.0
b0	0.43 ± 0.05	0.0012 ± 0.0003	0.0095 ± 0.0005	0.012 ± 0.003
b1	0.45 ± 0.05	0.0019 ± 0.0004	0.0100 ± 0.0004	0.024 ± 0.009
b2	0.39 ± 0.04	0.0028 ± 0.0006	0.0200 ± 0.0006	0.0
b3	0.49 ± 0.04	0.0025 ± 0.0005	0.0380 ± 0.0015	0.0
b4	0.42 ± 0.04	0.0029 ± 0.0005	0.0177 ± 0.0008	0.0
ea90_100				
pixel	kT	norm	O norm	N_2 norm*
a0	0.47 ± 0.05	0.00026 ± 0.00015	0.0018 ± 0.0002	0.0015 ± 0.0006
a1	0.42 ± 0.02	0.00120 ± 0.00040	0.0055 ± 0.0004	0.0077 ± 0.0043
a2	0.41 ± 0.02	0.00180 ± 0.00040	0.0045 ± 0.0003	0.0053 ± 0.0030
a3	0.42 ± 0.02	0.00184 ± 0.00038	0.0048 ± 0.0004	0.0100 ± 0.0060
a4	0.40 ± 0.03	0.00151 ± 0.00041	0.0095 ± 0.0005	0.0 ± 0.018
b0	0.43 ± 0.05	0.00041 ± 0.00020	0.0019 ± 0.0003	0.0019 ± 0.0015
b1	0.45 ± 0.05	0.00153 ± 0.00035	0.0021 ± 0.0003	0.0
b2	0.39 ± 0.04	0.00167 ± 0.00040	0.0041 ± 0.0003	0.0
b3	0.49 ± 0.04	0.00077 ± 0.00045	0.0072 ± 0.0006	0.0
b4	0.42 ± 0.04	0.00128 ± 0.00050	0.0035 ± 0.0004	0.0

*NOTE: The nitrogen line energy is fixed at 0.392 keV for all pixels except for a0 where the best fit is 0.386 ± 0.002 abd b0 where the best fit is 0.393 ± 0.003. The values in this table apply only when using the test18 matrix.

5 Procedure: Chi-square Analysis

For sources strong enough to use chi-square statistics, one can create a combined "best" background spectrum for each observation. For a night observation this consists of 1) the diffuse background minus its internal background plus 2) the internal background scaled to the source guard rate. For a day observation, 1) the daytime background for the appropriate Earth angle minus its internal background plus 2) an internal background scaled to the source guard rate. In each case the two files can be added together to make one background file for the observation which can be used in *xspec*. A program now exists which allows the user to subtract as well as add pha files and is called *fixpha*. All of the relevent background files necessary to create appropriate summed spectra are summarized in Table 4. File sets #1 and 3 are located in /home/chaupher/kim/back/INTERNAL_dir, file sets #2 and 4 are in /home/chaupher/kim/back/NIGHT_dir, and file sets #5,6 and 7 are in /home/chaupher/kim/back/DAY_dir/EAXX_XX (where EAXX_XX stands for the Earth angle range, i.e. EA90_100). The scaled internal backgrounds for both the nighttime diffuse background files and the daytime bright Earth have already been produced.

Table 4: Summary of available files

num	file name	background components
1	back855_2msXX.pha	internal (MGR=1259)
2	nightbackXX.pha	diffuse + internal
3	night_back855_2msXX.pha	internal scaled to MGR=1274
4	night_minus_int_backXX.pha	diffuse
5	eaXX_XXdaynsaaXX.pha	scattered + diffuse + internal
6	eaXX_XX_back855_2msXX.pha	internal scaled to eaXX_XX MGR
7	eaXX_XXdaynsaabackXX.pha	diffuse + scaled internal

6 Generating files

The following step by step method shows how to generate a combined background file for your observation.

For a night observation,

(1) Take *back855_2msXX.pha* and scale it to the MGR for a given source by changing the BSF using the algorithm

BSF = 1259/MGR for MGR > 1000

BSF = 1.259 for MGR < 1000

Call the resulting file *temp1_XX.pha*

(2) Take *night_minus_int_backXX.pha* and add it to *temp1_XX.pha* using *fixpha* and the result is your final NIGHT background spectrum.

For a day observation,

(1) Take the *eaXX_XXdaynsaaXX.pha* file relevent to the average Earth angle of your observation.

(2) Subtract from this the *eaXX_XX_back855_2msXX.pha* file using *fixpha*, and call this file *temp2_XX.pha* (this leaves you with one file containing the internal background and one containing the scattered plus diffuse).

EXAMPLE:

```
chaupher-210: fixpha
  Input file name: ea90_100daynsaaa0.pha
Bins 512, Time: 7330.11, Effective area: 1.00000
  Input file name: -ea90_100back855_2msa0.pha
Bins 512, Time: 8255.39, Effective area: 1.00000
  Input file name:
Output PHA file name: temp2_a0.pha
```

(3) add *temp2_XX.pha* to *temp1_XX.pha* using *fixpha* to get the final DAY background spectrum. No additional scaling is required.

The above applies to non-SAA observations only and is not guaranteed to work if your source MGR is too high (i.e. above 1,400).

Once an appropriate background file has been created, it is possible (at least for weak point sources) to test the accuracy of the subtraction by using a pixel which contains minimal source flux. This procedure has been used for a daytime observation of the Seyfert galaxy NGC 4051. A summed background file was created corresponding to the same average guard rate and Earth angle as the source. The source was offset enough in the detector that two pairs of outer pixels (a3/b1 and a4/b2) contained essentially no source counts. Figures 8a and b shows the residuals to a background subtraction for pixels a3 and b2 using the summed background file. The subtraction in this case works perfectly.

7 References

Bambynek, et al. 1972, Rev. Mod. Phys., 44, 716.

Bearden, J. A. 1967, Rev. Mod. Phys., 39, 78.

Bearden, J. A. and Burr, A. F. 1967, Rev. Mod. Phys., 39, 125.

Fink, H.H., Schmitt, J.H.M.M. and Harnden, F.R. 1988, Astron. Astr., 193, 345.

Gould, R. J. and Jung, Y. 1991, Ap.J., 373, 271.

Jahoda et al, 1991, contribution to *The International Workshop on the X-Ray Background*, eds. X. Barcons and A. C. Fabian (Cambridge: Cambridge University Press) p. 240.

Jones, L. M. 1964, contribution to the "University of Michigan Engineering Summer Conferences on High Altitude Science" (Ann Arbor: University of Michigan), pp. 1:2-1:25.

Marshall, F. 1991a, memo-"BBXRT Internal Background Study"

Marshall, F. 1991b, memo-"Subtracting Background for BBXRT"

Mitra, S. K. 1952, "The Upper Atmosphere," 2nd ed., (Calcutta: The Asiatic Society), p. 174.

Schmitt, J.H.M, Harnden. F.R. and Fink, H. 1987, Ap.J., 322, 1023.

Snowden, S.L., and Freyberg, M.J. 1993, Ap.J. (submitted)

Weaver, K. 1992, memo-"BBXRT Calibration Update"

Yamauchi, S. 1991, memo-"BBXRT Diffuse X-ray Emission"

Zombeck, M.V. 1990, "Handbook of Space Astronomy and Astrophysics", (Cambridge U. Press), pp. 239 and 243.

8 Figure Captions

Figure 1: Relative densities (cm^{-3}) of molecular and atomic oxygen in the Earth's atmosphere as a function of height between 90 and 140 km.

Figure 2: BBXRT Solar flare data illustrating the stronger high energy continuum and emission lines seen during a flare.

Figure 3: a) Quiescent Solar scattered spectrum for Earth angle range of 30-50 degrees. b) Quiescent Solar scattered spectrum for Earth angle range of 80-90 degrees. Both spectra are from pixel A2.

Figure 4: Change in daytime count rate (a2 pix) with Earth limb angle. a) Channels 27-42. b) Channels 45-80. c) Channels 80-120.

Figure 5: Internal background count rate vs. guard A rate. The y-axis represents the count rate for the summed outer A pixels, channels 51-511.

Figure 6: Internal background subtracted Pixel A1 count rate for daytime scattered background data (channels 16-60, Earth angle range 100-110 degrees) vs. guard rate.

Figure 7: Illustration of fits to the oxygen fluorescence line for all pixels for daytime data at Earth angles 100-110.

Figure 8: Residuals from subtracting a summed background from off-source NGC 4051 pixels. The background file was created by adding background subtracted daytime data (ea100-110) to a diffuse background file and a scaled internal background file.

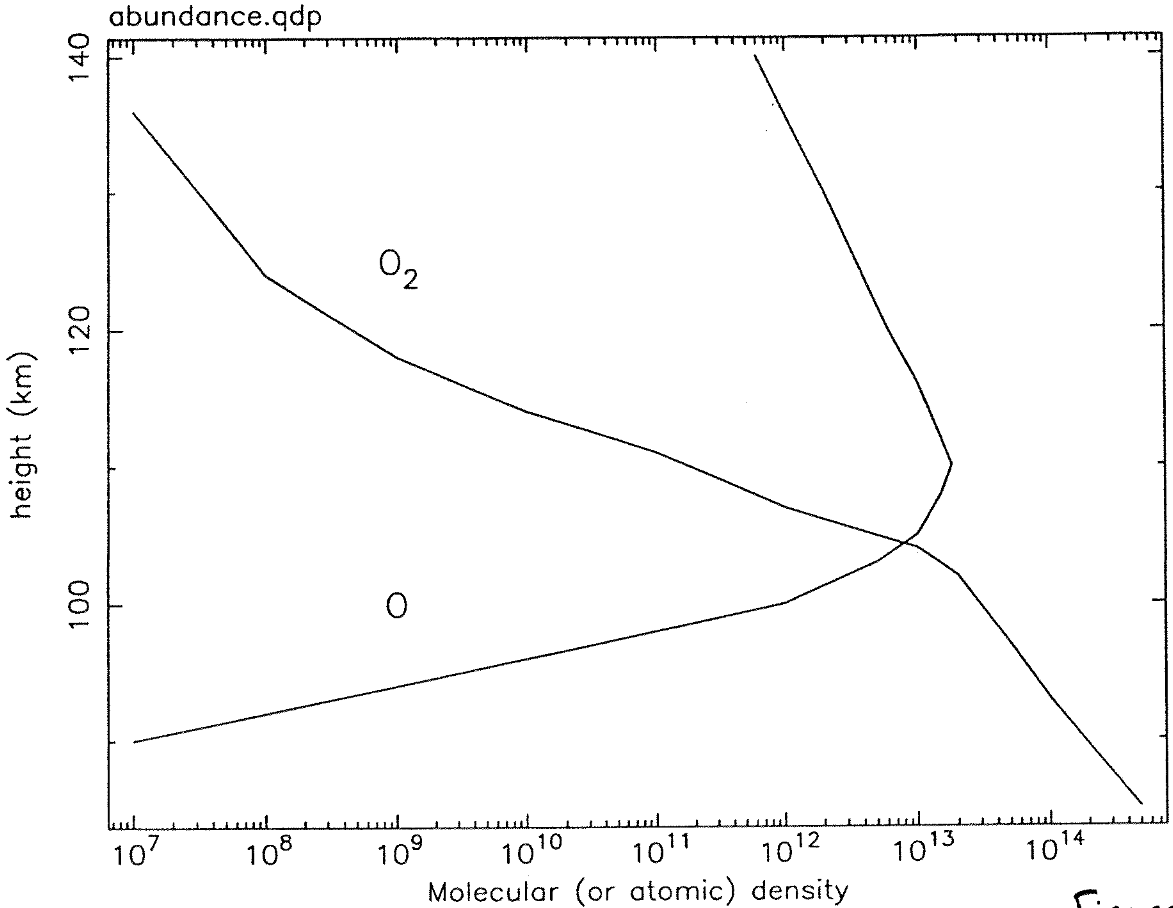

Figure 1

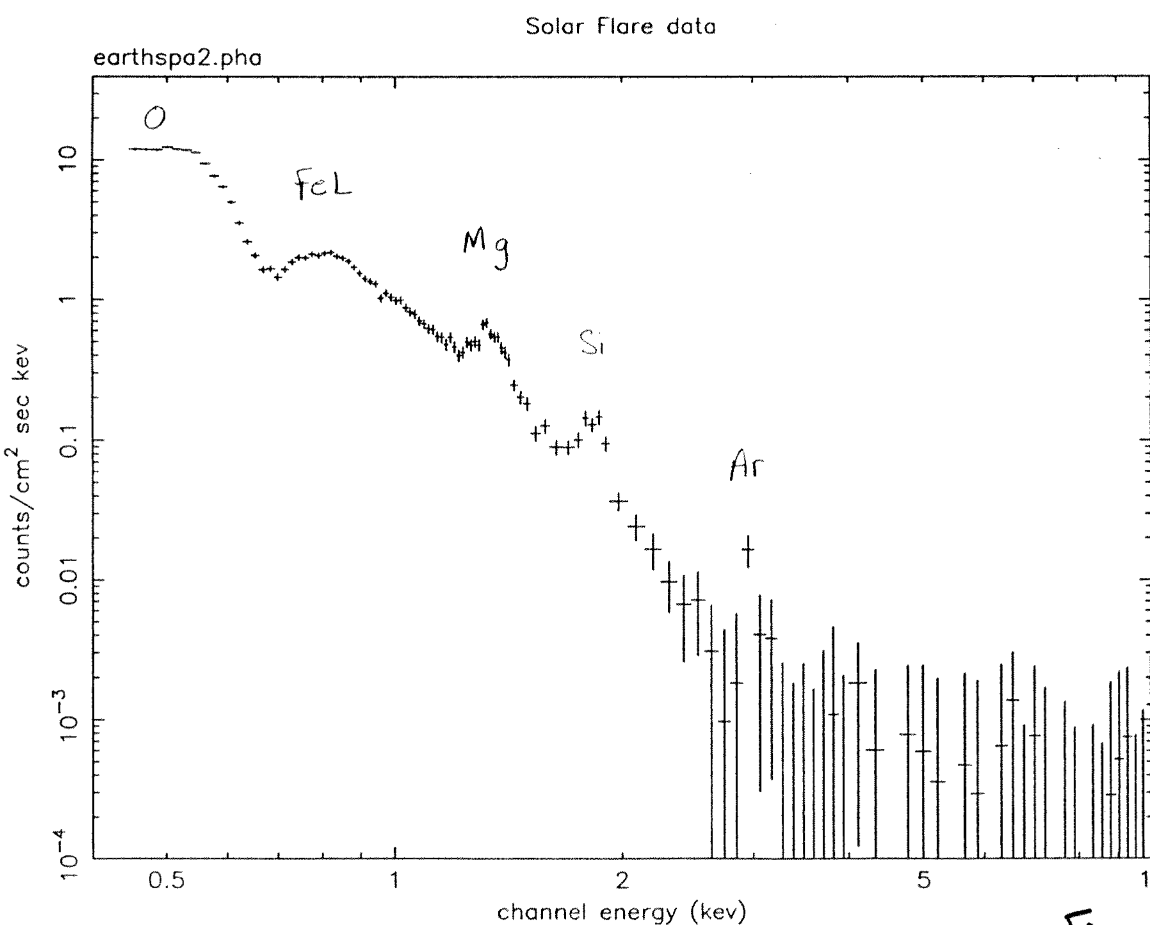

Figure 2

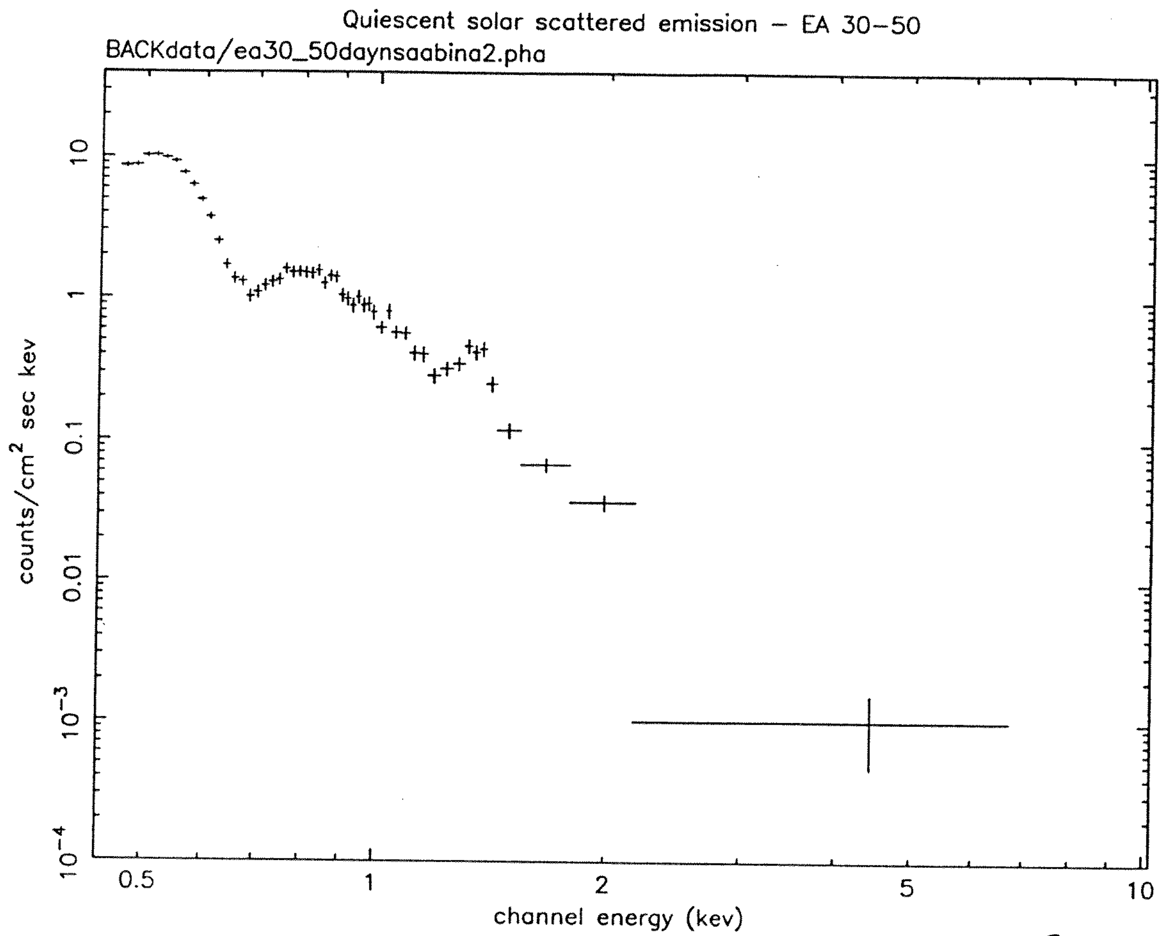

Figure 3a

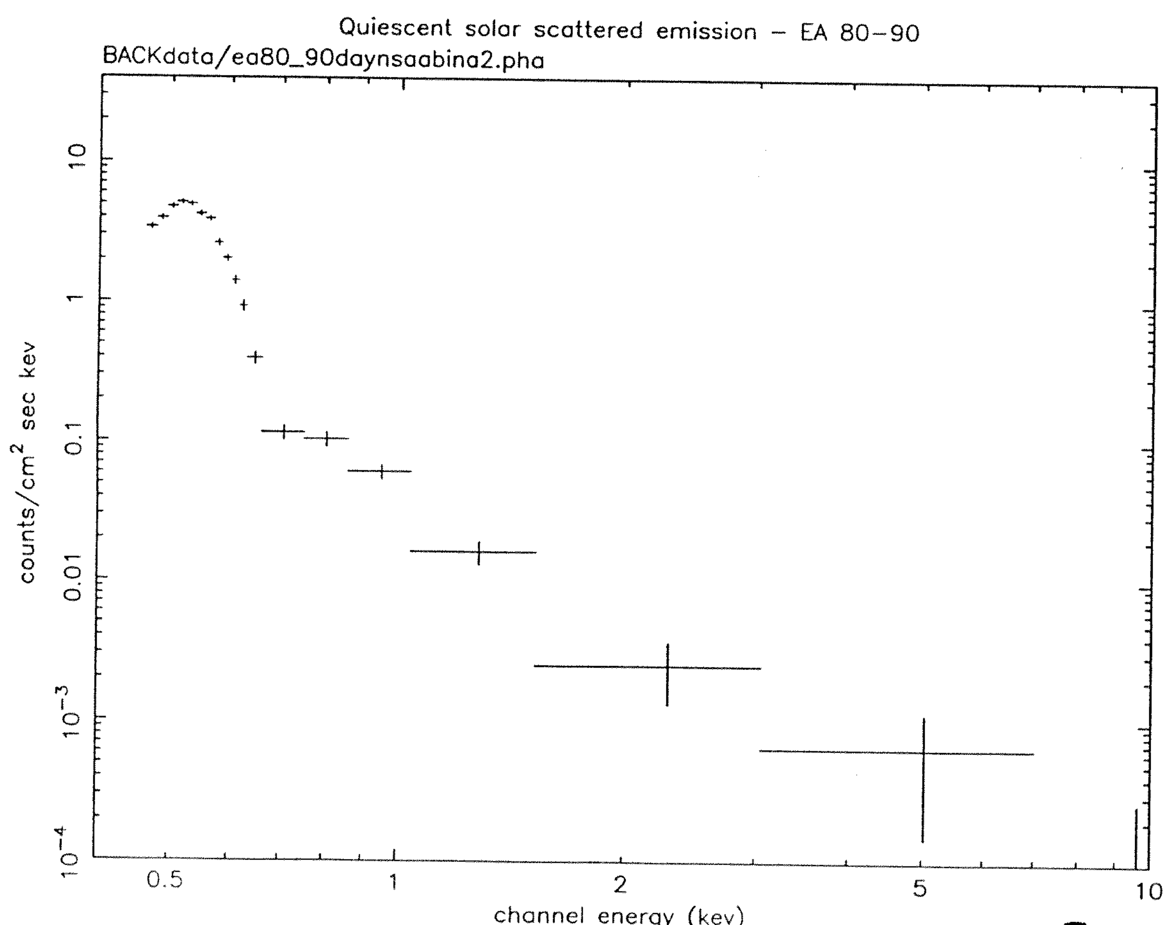

Figure 3b

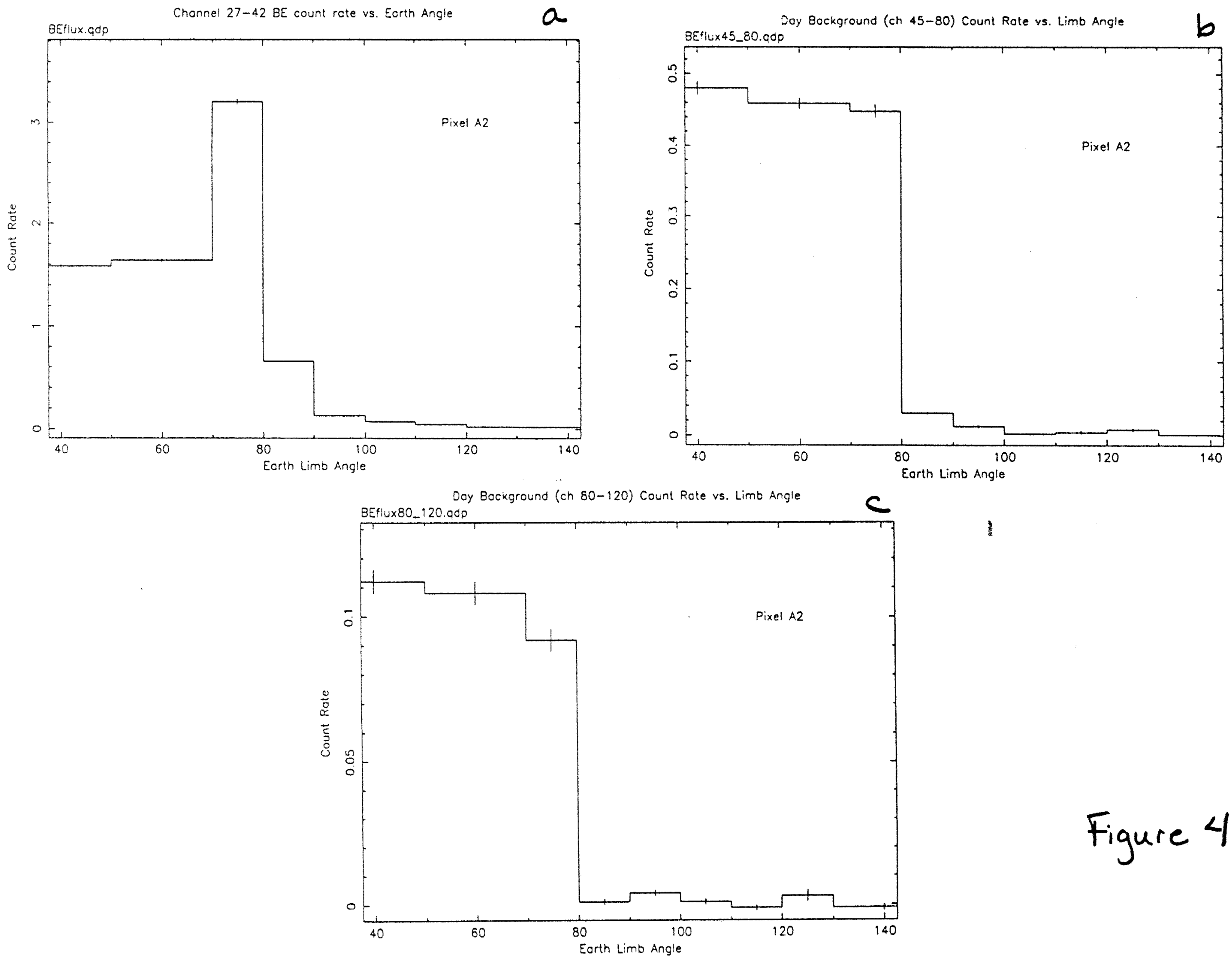

a
Channel 27-42 BE count rate vs. Earth Angle
BEflux.qdp
Pixel A2
Count Rate
Earth Limb Angle
0
1
2
3
40
60
80
100
120
140
b
Day Background (ch 45-80) Count Rate vs. Limb Angle
BEflux45_80.qdp
Pixel A2
Count Rate
Earth Limb Angle
0
0.1
0.2
0.3
0.4
0.5
40
60
80
100
120
140
c
Day Background (ch 80-120) Count Rate vs. Limb Angle
BEflux80_120.qdp
Pixel A2
Count Rate
Earth Limb Angle
0
0.05
0.1
40
60
80
100
120
140

Figure 4

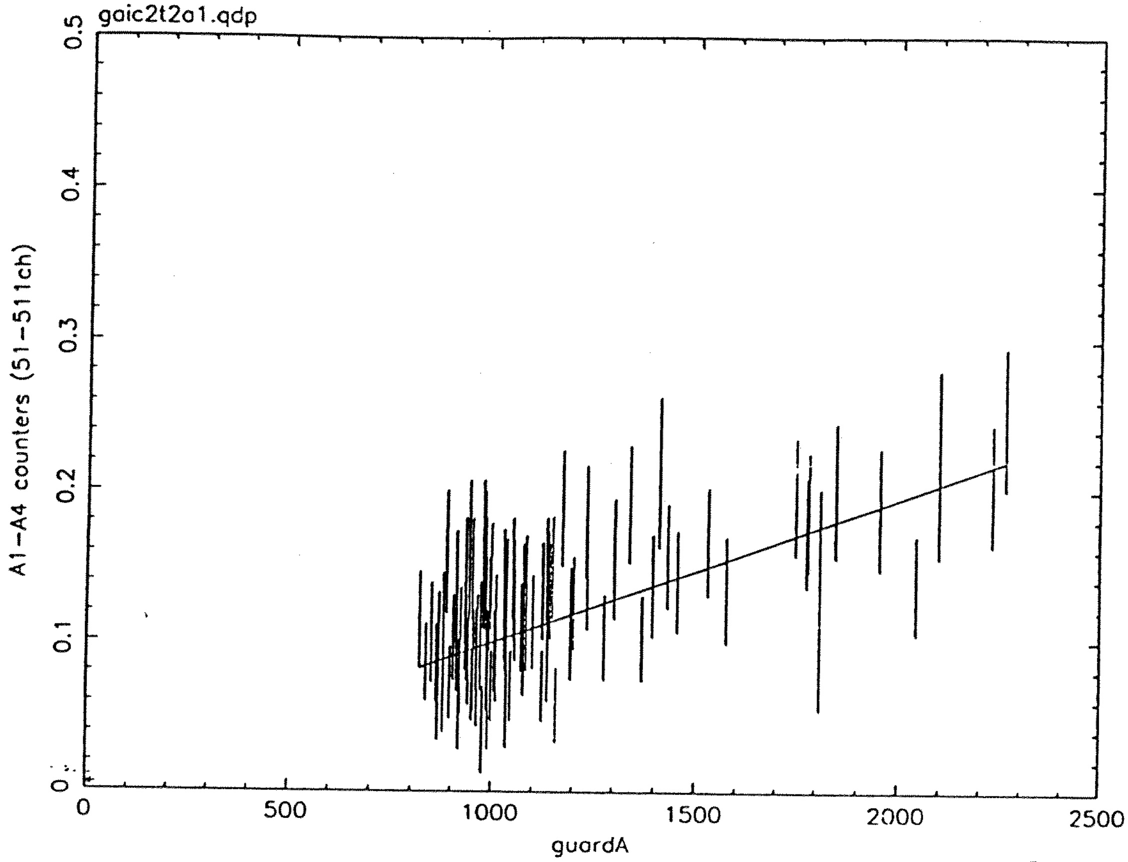

Figure 5

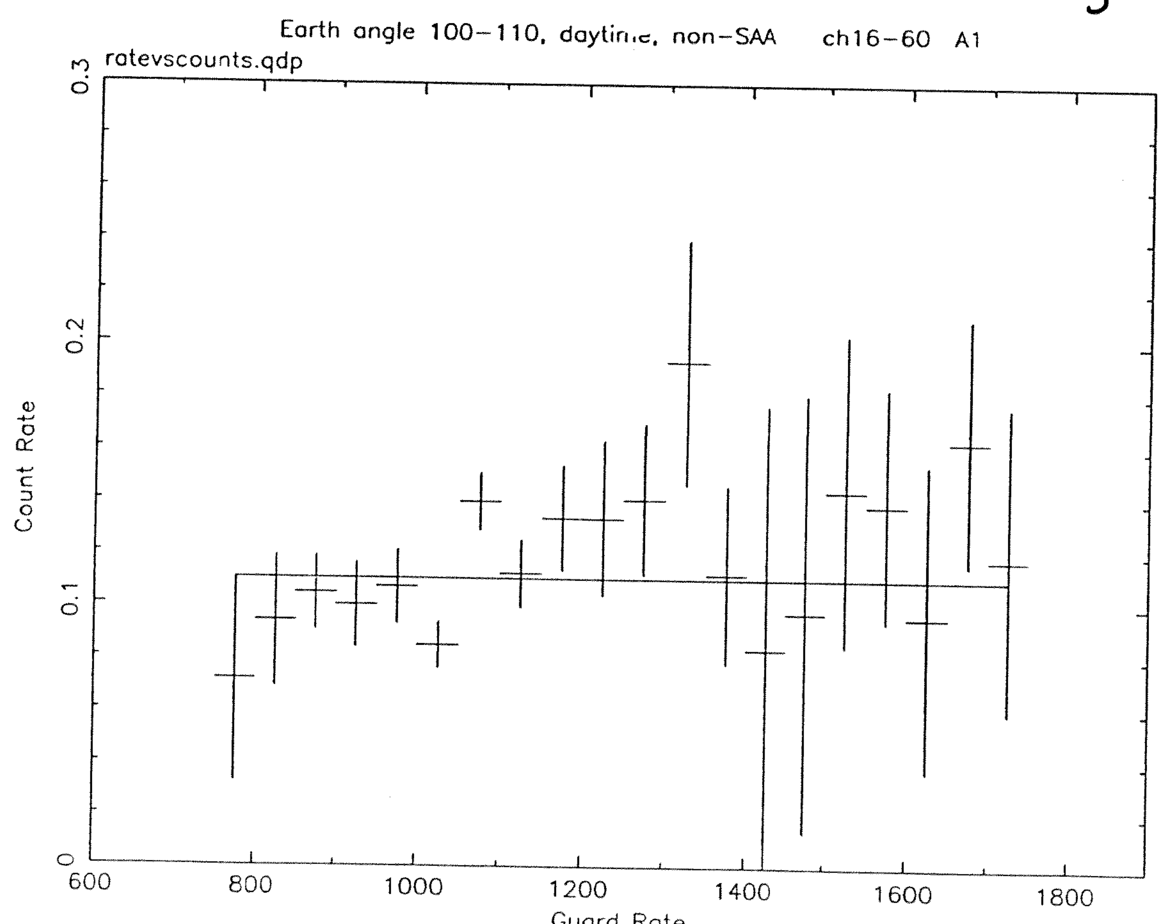

Figure 6

Figure 7

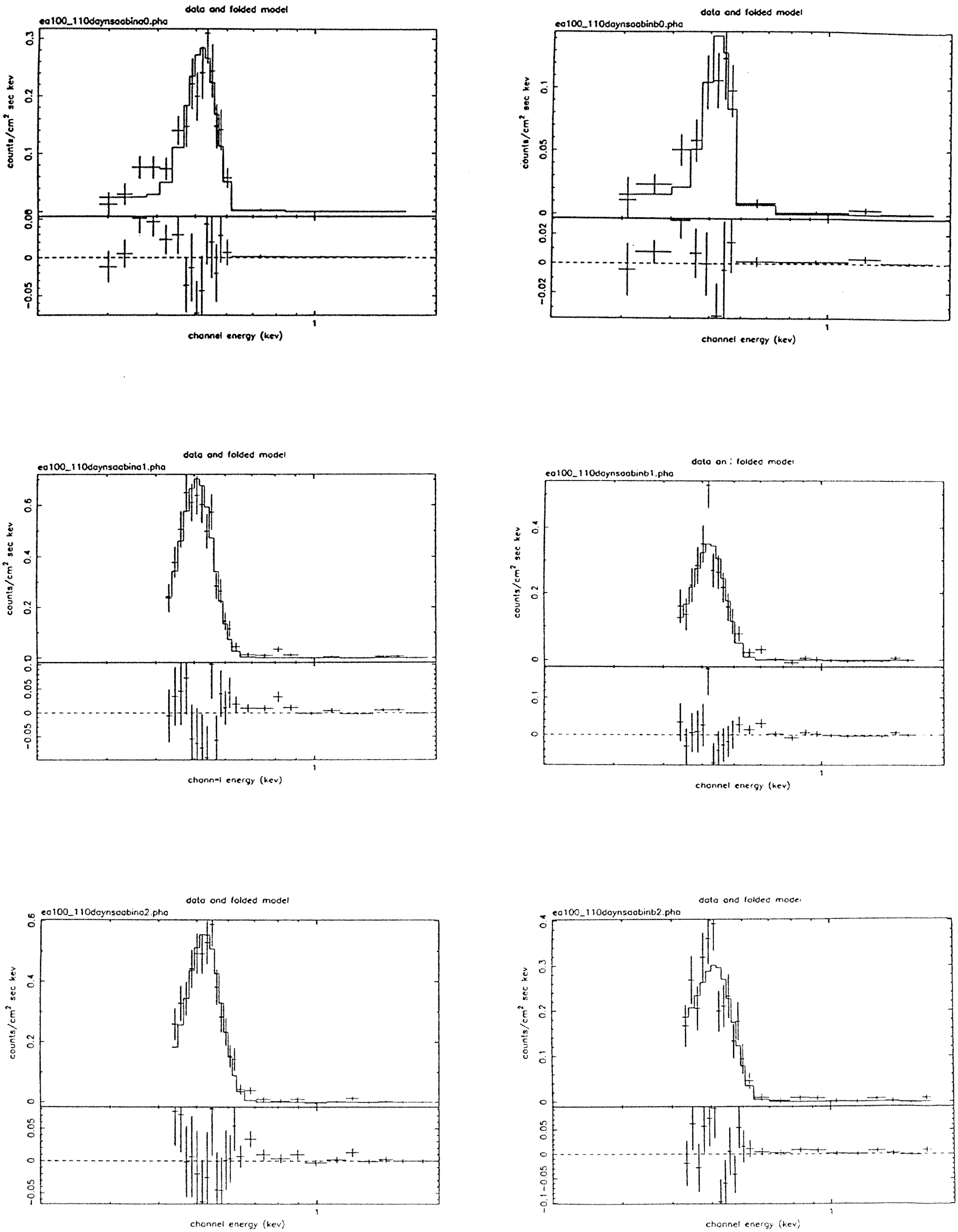
data and folded model
ea100_110daynsaabina0.pha
counts/cm2 sec kev
channel energy (kev)
data and folded model
ea100_110daynsaabinb0.pha
counts/cm2 sec kev
channel energy (kev)
data and folded model
ea100_110daynsaabina1.pha
counts/cm2 sec kev
channel energy (kev)
data and folded model
ea100_110daynsaabinb1.pha
counts/cm2 sec kev
channel energy (kev)
data and folded model
ea100_110daynsaabina2.pha
counts/cm2 sec kev
channel energy (kev)
data and folded model
ea100_110daynsaabinb2.pha
counts/cm2 sec kev
channel energy (kev)

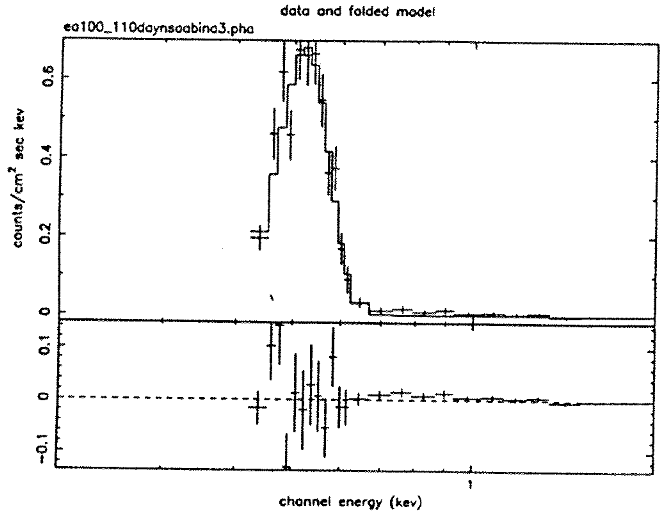
data and folded model
ea100_110daynsaabina3.pha
counts/cm^2 sec kev
0.6
0.4
0.2
0
0.1
0
−0.1
1
channel energy (kev)

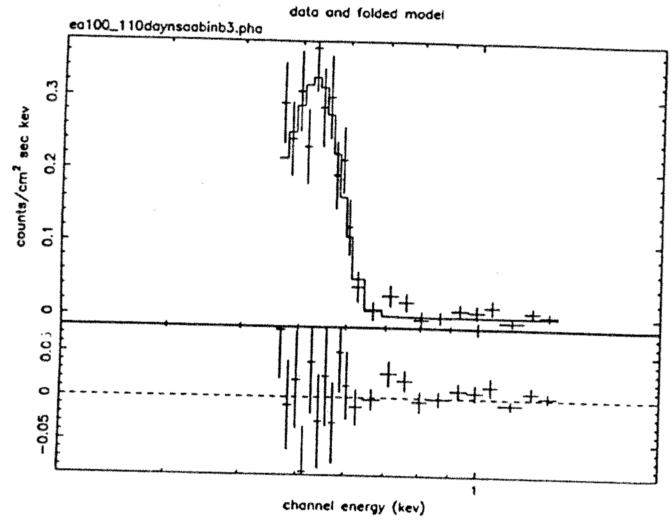
data and folded model
ea100_110daynsaabinb3.pha
counts/cm^2 sec kev
0.3
0.2
0.1
0
0
−0.05
1
channel energy (kev)

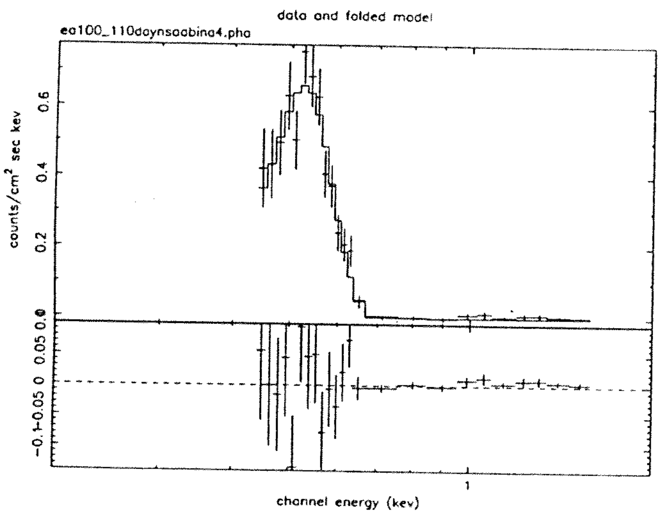
data and folded model
ea100_110daynsaabina4.pha
counts/cm^2 sec kev
0.6
0.4
0.2
0.0
0.05
0
−0.1−0.05
1
channel energy (kev)

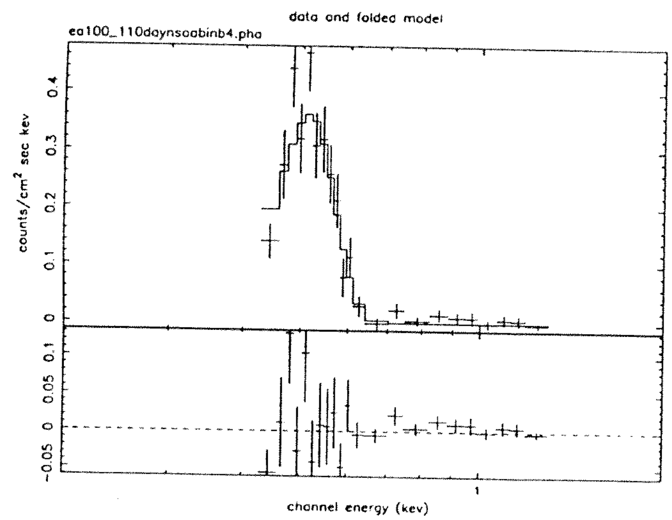
data and folded model
ea100_110daynsaabinb4.pha
counts/cm^2 sec kev
0.4
0.3
0.2
0.1
0
0.1
0.05
0
−0.05
1
channel energy (kev)

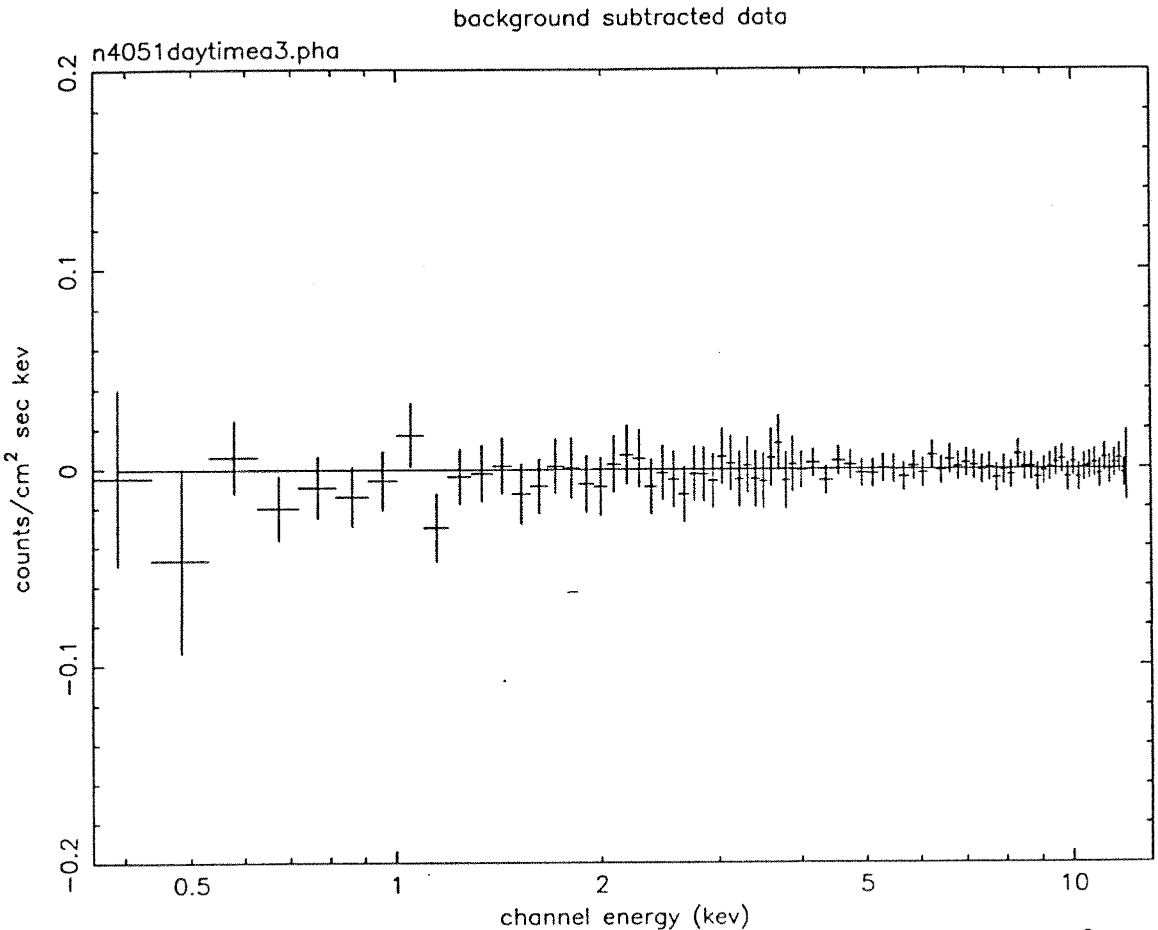

Figure 8a

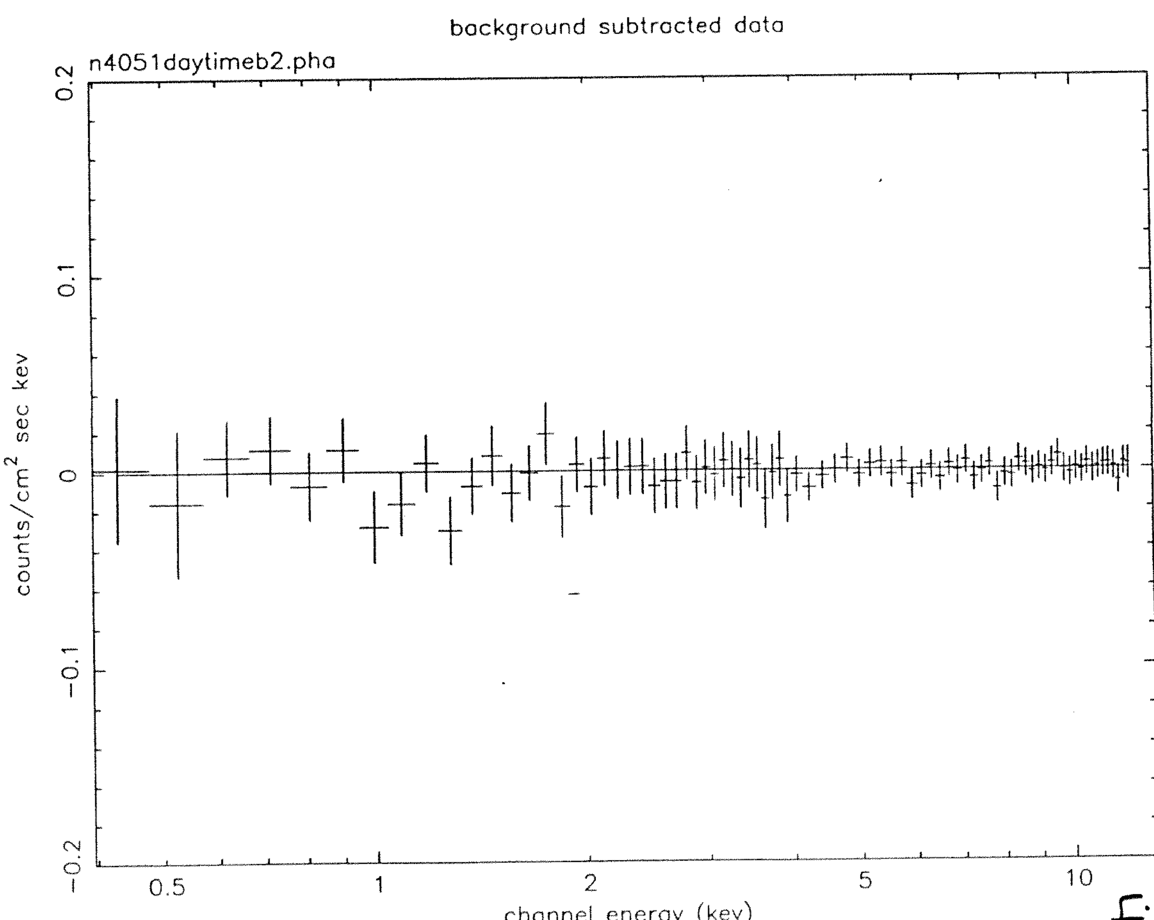

Figure 8b